J. Shanghai Jiao Tong Univ. (Sci.), 2023
https://doi.org/10.1007/s12204-023-2633-8

Adjacent Segment Biomechanical Changes After Implantation of Cage Plus Plate or Zero-Profile Device in Different Segmental Anterior Cervical Discectomy and Fusion

YE Peng (叶　鹏), *FU Rongchang** (富荣昌), *WANG Zhaoyao* (王召耀)
(School of Mechanical Engineering, Xinjiang University, Urumqi 830017, China)

Abstract: Cage plus plate (CP) and zero-profile (Zero-P) devices are widely used in anterior cervical discectomy and fusion (ACDF). This study aimed to compare adjacent segment biomechanical changes after ACDF when using Zero-P device and CP in different segments. First, complete C1—C7 cervical segments were constructed and validated. Meanwhile, four surgery models were developed by implanting the Zero-P device or CP into C4—C5 or C5—C6 segments based on the intact model. The segmental range of motion (ROM) and maximum value of the intradiscal pressure of the surgery models were compared with those of the intact model. The implantation of CP and Zero-P devices in C4—C5 segments decreased ROM by about 91.6% and 84.3%, respectively, and increased adjacent segment ROM by about 8.3% and 6.82%, respectively. The implantation of CP and Zero-P devices in C5—C6 segments decreased ROM by about 93.3% and 89.9%, respectively, while increasing adjacent segment ROM by about 4.9% and 4%, respectively. Furthermore, the implantation of CP and Zero-P devices increased the intradiscal pressure in the adjacent segments of C4—C5 segments by about 4.5% and 6.7%, respectively. The implantation of CP and Zero-P devices significantly increased the intradiscal pressure in the adjacent segments of C5—C6 by about 54.1% and 15.4%, respectively. In conclusion, CP and Zero-P fusion systems can significantly reduce the ROM of the fusion implant segment in ACDF while increasing the ROM and intradiscal pressure of adjacent segments. Results showed that Zero-P fusion system is the best choice for C5—C6 segmental ACDF. However, further studies are needed to select the most suitable cervical fusion system for C4—C5 segmental ACDF. Therefore, this study provides biomechanical recommendations for clinical surgery.
Key words: biomechanics, finite element analysis, adjacent segment degeneration, range of motion (ROM), intradiscal pressure
CLC number: R 318.01　　**Document code:** A

0 Introduction

Cervical spondylosis is characterized by the compressed cervical spinal cord, nerve roots, or vertebral arteries due to long-term cervical strain, osteophytes, or disc prolapse, resulting in various functional disorders[1]. Although anterior cervical discectomy and fusion (ACDF) is considered the gold treatment of cervical spine disorders[2], it is associated with adjacent segment degeneration (ASD)[3]. Studies have shown that ASD may be caused by an abnormal segmental range of motion (ROM) and intradiscal pressure[4]. Results of biomechanical study suggest that ASD is caused by excessive activity and increased stress in adjacent segments after cervical fusion cage system is implanted, which leads to accelerated degeneration of these segments[5].

Although the cage plus plate (CP) fusion system is widely used in ACDF, it increases the risk of postoperative complications, such as postoperative dysphagia, tracheoesophageal lesions, and ASD[6]. As a result, a zero-profile (Zero-P) device has been developed to avoid the possible irritation of adjacent segments caused by the plate used in the CP fusion system[7]. Zhang et al.[8] showed that CP and Zero-P systems have similar clinical and radiological outcomes after ACDF based on the incidence of postoperative ASD. However, they did not determine the biomechanical properties of the adjacent segments after using the two fusion systems in ACDF.

Hua et al.[9] constructed a finite element cervical spine model consisting of C2—C7 segments and compared the biomechanical properties of the adjacent segments using one- or two-level CP and Zero-P devices implanted in the same segment. Similarly, they did not

Received: 2022-09-26　**Accepted:** 2023-03-08
Foundation item: the National Natural Science Foundation of China (Nos. 32260235 and 82260446)
∗**E-mail:** 2781642414@qq.com

determine the biomechanical properties of adjacent segments after the implantation of different systems. In this study, a complete model of the finite element cervical spine consisting of C1—C7 was constructed, and then two fusion systems (CP and Zero-P devices) were implanted between the two segments with high clinical morbidity. The ROM of adjacent segments and the intradiscal pressure of the cervical spine were analyzed under three conditions, including flexion extension, lateral flexion, and axial rotation. Therefore, this study may provide a theoretical basis for the biomechanical causes of ASD and a technical guide for the mechanical aspects of the ACDF procedure.

1 Materials and Methods

1.1 Establishment of an Intact Cervical Spine C1—C7 Model

A 24-year-old male with a height of 181 cm, body mass of 67 kg, without a history of trauma to the neck, and without cervical spine disease (based on X-ray examination) volunteered for the study. This study was approved by the ethics committee of the School of Mechanical Engineering, Xinjiang University, and the subject signed the relevant informed consent form. A CT scanner was used to scan the male volunteer's cervical spine. Set the scanning layer thickness to 1 mm and the layer spacing to 1 mm in the scanning process. The whole head and neck scanning process was performed by professional scanning technicians in the department. A total of 843 images in DICOM format were obtained and saved. The DICOM files were imported into Mimics (Materialise Inc., Leuven, Belgium) for the reconstruction of a 3D model of each vertebra. Spatial geometry of the cervical vertebrae was then recovered and reproduced. Smooth and geometrically sound 3D vertebrae were constructed in Mimics using threshold segmentation, region growing, erasing, editing, and smoothing and exported as STL files. The STL files were further processed in FreeForm Modeling Plus (3D Systems, Inc., SC, USA) and Geomagic Studio 2012 (Geomagic, Inc., NC, USA) for the construction of the solid model and exported as IGES files. The IGES file was imported in Hypermesh 14.0 (Altair Engineering, Inc., Troy, MI, USA), and the complete solid model of the cervical spine was meshed. In the finite element analysis, the vertebral body of the cervical spine can be divided into cortical bone, cancellous bone, endplate and posterior structure. The cortical bone was simulated by triangular shell unit (thickness is 1 mm). The cancellous bone was simulated by mixed tetrahedral and pentahedral unit, while the endplate was simulated by rectangular unit. The fibrous ring matrix, nucleus pulposus, and cartilage were simulated by eight-node hexahedral unit. The ligament was only under tension and not compression, and was simulated by a 1D rod truss unit. It includes anterior longitudinal ligament, posterior longitudinal ligament, ligamentum flavum, interspinal ligament, joint capsule ligament and posterior capsule ligament. The location of ligaments is determined according to anatomy[10-12].

1.2 Fusion System Design and Modeling

The plate in the CP fusion system is made of medical titanium alloy. The plate has a height of 5 mm from the adjacent disc to prevent bone impingement with the anterior edge of the adjacent vertebral body[13]. The intraoperative ACDF screws using the CP fusion system should have an outward dispersion of 32° in the sagittal plane and an inward coalescence of 6° in the transverse plane to maintain the stability of the fusion system. Zero-P fusion system consists of an anterior titanium plate, a posterior PEEK interbody fusion, and interbody screws with four locking screw holes in the titanium plate with fixed angles to allow the screws to be locked to their cephalad/caudal side at an angle of 40° and to their medial/external side at 2.5°[14]. In this study, the cancellous bone screws (length is 14 mm and diameter is 3.5 mm) were used in both fusion devices. A simplified model without threads was used in the modeling process (material is medical titanium alloy)[15].

Several studies have shown that the prevalence of cervical spondylosis is higher in C4—C5 and C5—C6 segments than in other segments. Therefore, fusion implantation was simulated into these two segments[16]. The two anterior internal fixation systems in the intervertebral body were designed and assembled using SolidWork 2014 (SolidWorks Corp., MA, USA) to simulate the surgical implantation process and generate solid models. The screw, fixation plate, fusion, and implant in the Hypermesh were all linearly elastic isotropic materials. The established model is shown in Fig. 1.

The normal human cervical spine model and the models of the two fusion devices implanted in different segments were imported into the finite element calculation software ABAQUS 14.0 (Simulia, Inc., Rhode Island, USA), and the cell type and material properties were assigned. The material properties of each component and the cell selection were determined based on the selection in literature. The detailed parameters are shown in Table 1[17-22].

1.3 Boundary and Loading Conditions

In the C1—C7 model of the intact cervical spine and the CP and Zero-P implantation models, the C1 vertebral body center of mass was extracted to prevent artificial stress concentration caused by concentrated force loading[9]. Furthermore, the center of the mass point was coupled to the C1 vertebral body to ensure that the concentrated force was uniformly dispersed to the surface of the vertebral body[11]. The mass of the human head is generally 7% of the body mass. According to the body mass of volunteers, a 46.9 N concentrated

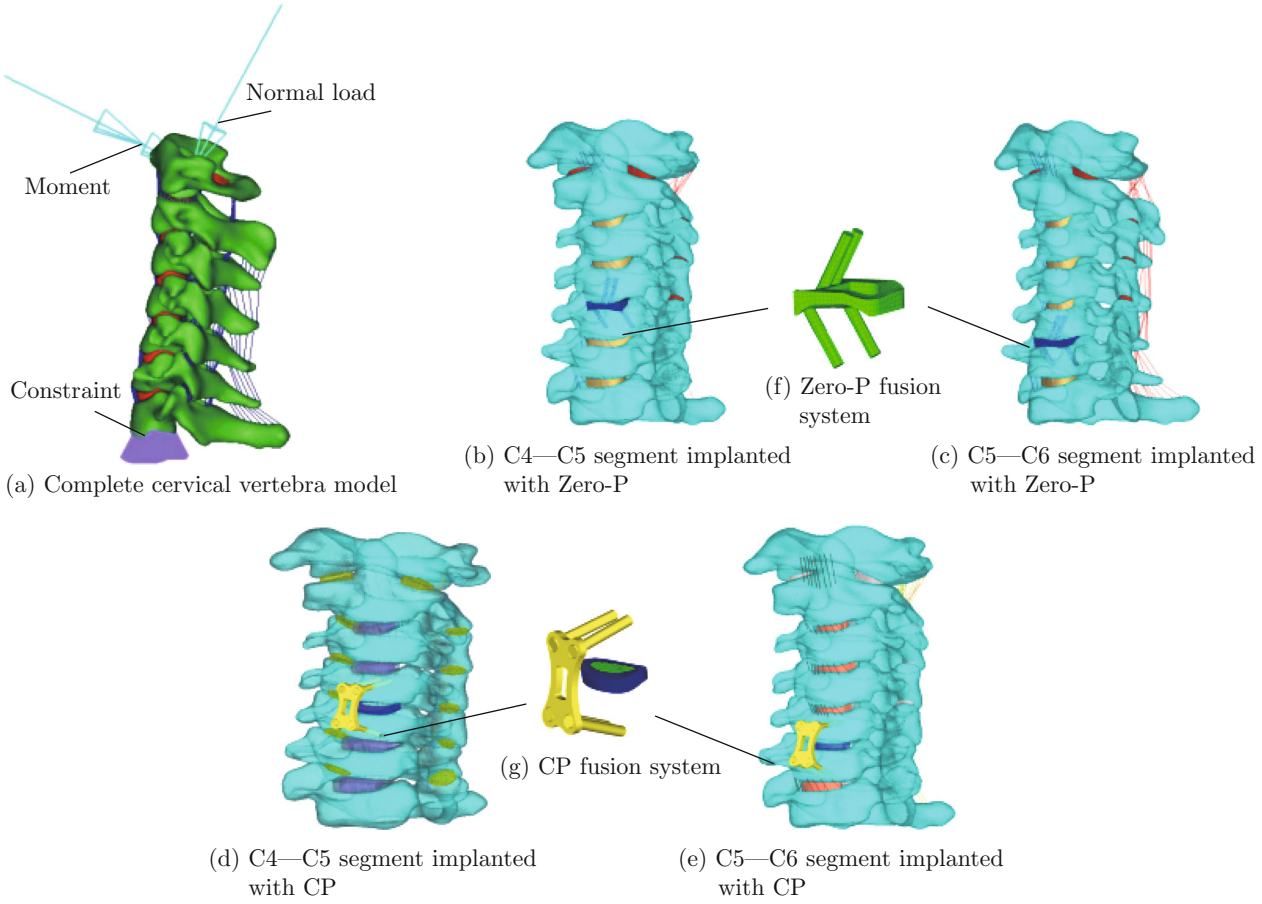

Fig. 1 Complete C1—C7 cervical vertebra model and the model implanted with fusion

Table 1 Unit selection and material parameters of each part of the cervical spine model

Model structure	Element type	Elastic modulus/MPa	Poisson's ratio	Cross-sectional area/mm^2
Cortical bone	S4R/S3	10 000	0.3	—
cancellous bone	C3D8R/C3D4	100	0.4	—
Endplate	S4R	450	0.4	—
Fibrous ring matrix	C3D8R	3.4	0.4	—
Medullary nucleus	C3D8R	1	0.49	—
Articular cartilage	C3D8R	10.4	0.4	—
Anterior longitudinal ligament (ALL)	T3D2	30	0.4	6.1
Posterior longitudinal ligament (PLL)	T3D2	20	0.4	5.4
Ligamentum flavum (LF)	T3D2	10	0.4	50.1
Interspinous ligament (ISL)	T3D2	10	0.4	13.1
Capsule ligament (CL)	T3D2	20	0.4	50.1
Fusions	C3D8R	3 600	0.31	—
Bone graft	C3D8R	3 500	0.3	—
Titanium	C3D8R	110 000	0.32	—

force was applied at the center of mass, the load direction was vertical downward, and 1.0 N · m torque was applied in different directions to simulate the anterior and posterior flexion and extension, left and right lateral flexion, and left and right rotation of the cervical spine[23]. The three physiological motion states were simulated. The lower surface of the C7 vertebral body of the above five finite element models was fully constrained and subjected to finite element analysis and calculation. The ROM of each segment of the complete cervical spine finite element model was analyzed under different motion modes and compared with previous

literature to verify the validity of the model.

2 Results

2.1 Model Validation

The complete cervical spine model established was analyzed using finite element analysis. The results were then compared with the human cadaveric cervical spine experiments conducted by Panjabi et al.[23] and the cervical spine model (including the skull) established by Zhang et al.[24] to validate the model. The results of the mobility of each segment under different working conditions and motion patterns are shown in Fig. 2. The cervical spine finite element calculation model was consistent with the overall cervical spine motion trend of ROM obtained from the previous solid experiments and simulation results.

2.2 Comparison of Segmental Mobility After Implantation of Fusion Devices in Different Segments

The ROMs of the adjacent segments and the implanted segments after the implantation of CP and Zero-P fusion systems are shown in Tables 2 and 3. The implantation significantly decreased the ROM of the segment compared with the intact model and increased the ROM of the adjacent segments.

Compared with the C4—C5 segments of the intact cervical spine model, the implantation of CP and Zero-P devices reduced the ROM in flexion-extension by 92.6% and 87.1%, respectively; in lateral flexion by

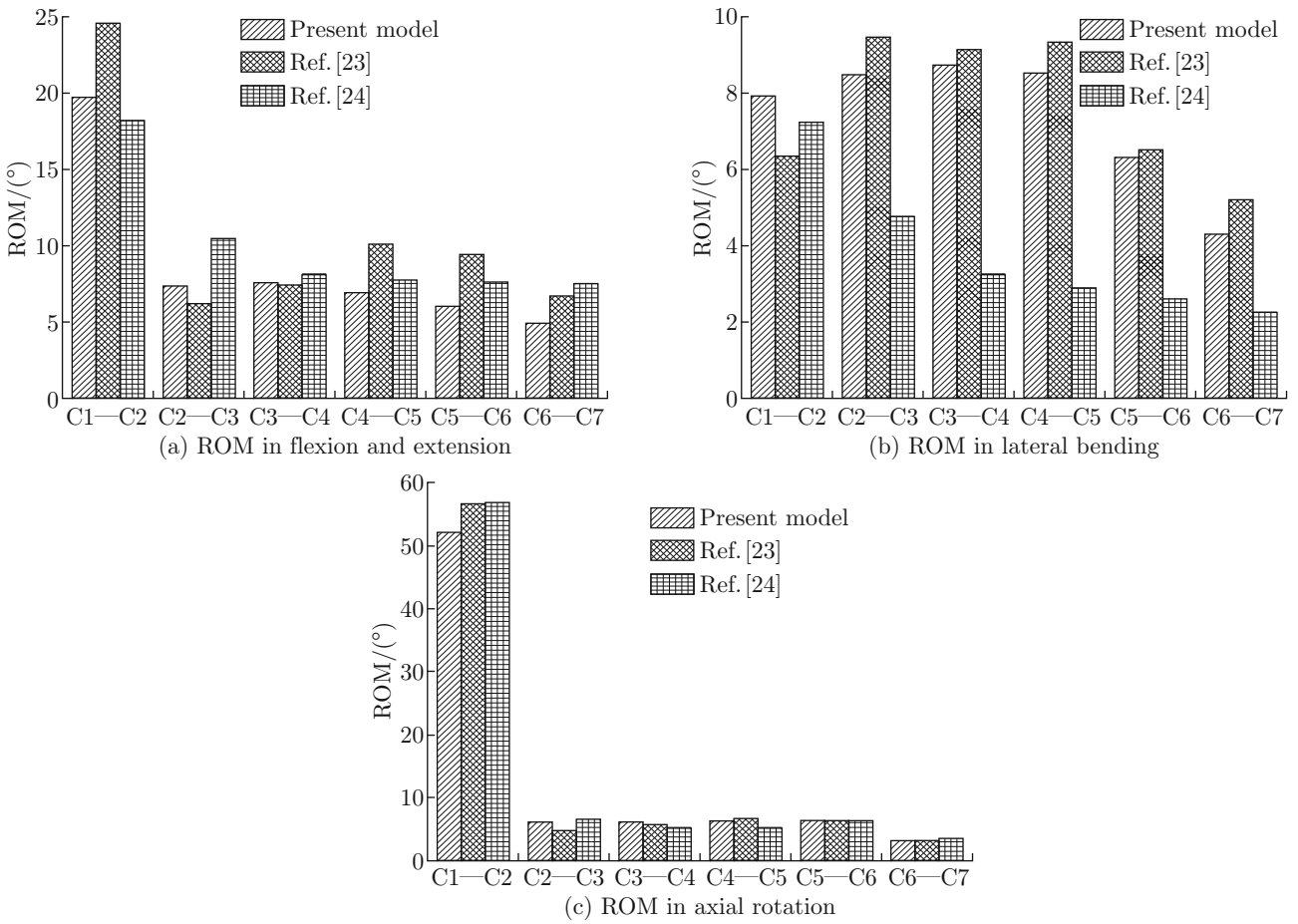

Fig. 2 Comparison of each segment ROM of C1—C7

Table 2 Comparison of ROMs after implantation of CP and Zero-P systems cage in C4—C5 (°)

Segment	Flexion-extension			Lateral bending			Axial rotation		
	Normal	CP	Zero-P	Normal	CP	Zero-P	Normal	CP	Zero-P
C3—C4	7.63	8.76	8.34	8.72	8.96	8.94	6.14	6.38	6.54
C4—C5	6.89	0.51	0.89	8.52	0.65	1.21	6.28	0.64	1.23
C5—C6	6.11	6.88	6.54	6.32	6.68	6.62	6.33	6.96	7.02

Table 3 Comparison of ROMs after the implantation of CP and Zero-P devices in C5—C6 (°)

Segment	Flexion-extension			Lateral bending			Axial rotation		
	Normal	CP	Zero-P	Normal	CP	Zero-P	Normal	CP	Zero-P
C4—C5	6.89	7.61	7.23	8.52	8.65	8.54	6.28	6.39	6.42
C5—C6	6.11	0.46	0.61	6.32	0.48	0.73	6.33	0.31	0.56
C6—C7	4.98	5.16	5.12	4.31	4.56	4.44	3.12	3.31	3.45

92.4% and 85.5%, respectively; and in axial rotation by 89.8% and 80.4%, respectively (Table 2). Furthermore, the implantation of CP and Zero-P devices increased the ROM of the adjacent segments for C3—C4 by 14.8% and 9.3% in flexion-extension, respectively; 2.8% and 2.5% in lateral flexion, respectively; and 3.9% and 6.5% in axial rotation, respectively (compared with the intact model). The implantation of CP and Zero-P devices also increased the ROM of the adjacent segments for C5—C6 by 12.6% and 7.0% in flexion-extension, respectively; 5.7% and 4.7% in lateral flexion, respectively; and 10% and 10.9% in rotation, respectively (compared with the intact model). In summary, the implantation of CP and Zero-P devices increased the ROM in the adjacent segments by about 8.3% and 6.28%, respectively.

Compared with the intact cervical spine model in the C5—C6 segments, the implantation of CP and Zero-P devices reduced the ROM by 92.5% and 90% in flexion-extension, respectively; by 92.4% and 88.4% in lateral flexion, respectively; and by 95.1% and 91.2% in axial rotation, respectively (Table 3). Furthermore, the implantation of the fusion system caused changes in the ROM of adjacent segments. The implantation of CP and Zero-P devices increased the ROM in the adjacent segments of C4—C5 by 10.4% and 4.9% in flexion-extension, respectively; by 1.5% and 0.23% in lateral flexion, respectively; and by 1.8% and 2.2% in axial rotation, respectively (compared with the intact model). The implantation of CP and Zero-P devices increased the ROM in the adjacent segments of C6—C7 by 3.6% and 2.8% in flexion-extension, respectively; by 5.8% and 3% in lateral flexion, respectively; and by 6.1% and 10.6% in axial rotation, respectively (compared with the intact model). In summary, the implantation of CP and Zero-P devices increased the ROM in the adjacent segments by about 4.9% and 4%, respectively.

2.3 Comparison of Intradiscal Pressure in Adjacent Segments After Implantation of Fusion Devices at Different Segments

The implantation of CP and Zero-P devices in the C4—C5 segments increased the intradiscal pressure in both C3—C4 and C5—C6 adjacent segments (Table 4 and Fig. 3). For the C3—C4 segments, CP and Zero-P devices increased the intradiscal pressure by 1.4% and 2.1% in flexion-extension, respectively; by 3.5% and 4.7% in lateral flexion, respectively; and by 8.6% in axial rotation (compared with the intact model). For the C5—C6 segments, CP and Zero-P devices increased the intradiscal pressure by 0.7% and 3.6% in flexion-extension, respectively; by 11.5% and 16.1% in lateral flexion, respectively; and by 1% and 5.2% in axial rotation, respectively (compared with the intact model). In summary, the implantation of CP and Zero-P devices into C4—C5 increased the intradiscal pressure in the adjacent segments by about 4.5% and 6.7%, respectively.

The implantation of CP and Zero-P devices in the C5—C6 segments increased the intradiscal pressures in the adjacent C4—C5 and C6—C7 segments (Table 5 and Fig. 4). For the C4—C5 segments, CP and Zero-P devices increased the intradiscal pressures by 20.1% and 5.9% in flexion-extension, respectively; by 26.9% and 14.4% in lateral flexion, respectively; and by 27% and 18% in axial rotation, respectively (compared with the intact model). For the C6—C7 segments, CP and Zero-P devices increased the intradiscal pressures by 71.3% and 18.5% in flexion-extension, respectively; by 90.5%, 13.5% in lateral flexion, respectively; and by 88.9% and 22.2% in axial rotation, respectively (compared with the intact model). In summary, the implantation of CP and Zero-P devices into C5—C6 increased the intradiscal pressure in the adjacent segments by about 54.1% and 15.4%, respectively.

Table 4 Intradiscal pressure in adjacent segments after implantation of CP and Zero-P devices in C4—C5

MPa

Segment	Flexion-extension			Lateral bending			Axial rotation		
	Normal	CP	Zero-P	Normal	CP	Zero-P	Normal	CP	Zero-P
C3—C4	1.43	1.45	1.46	0.85	0.88	0.89	0.81	0.88	0.88
C4—C5	1.69	—	—	1.04	—	—	1.00	—	—
C5—C6	1.37	1.38	1.42	0.87	0.97	1.01	0.96	0.97	1.01

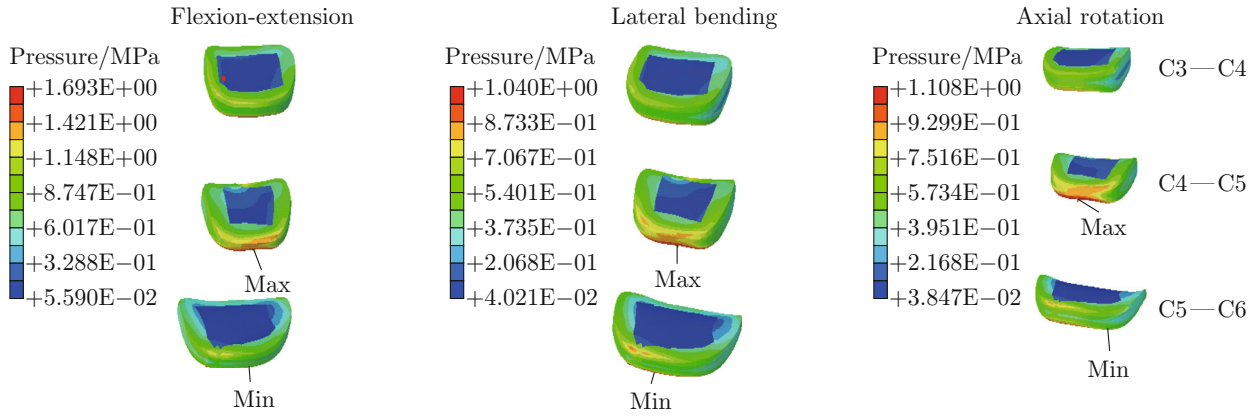

(a) Stress cloud plots showing the condition at intact cervical spine

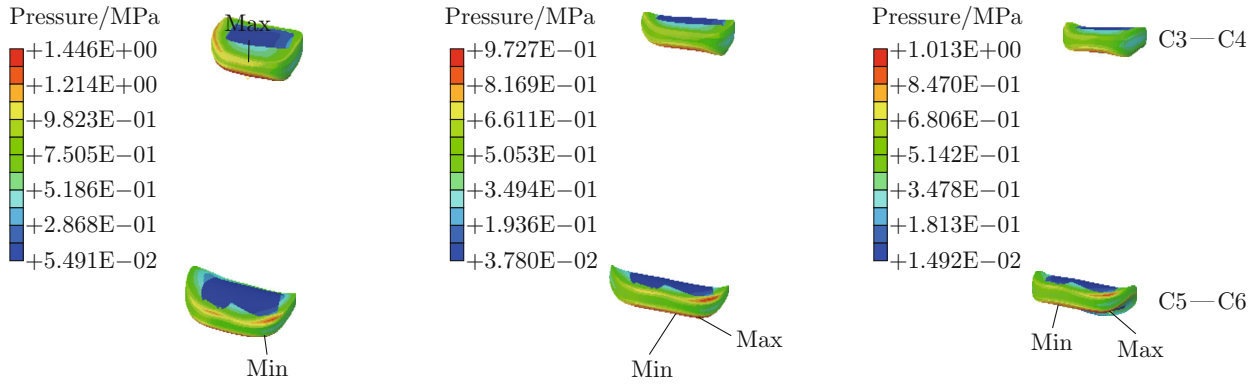

(b) Stress cloud plots showing the condition at the C4—C5 segments implanted with CP fusion

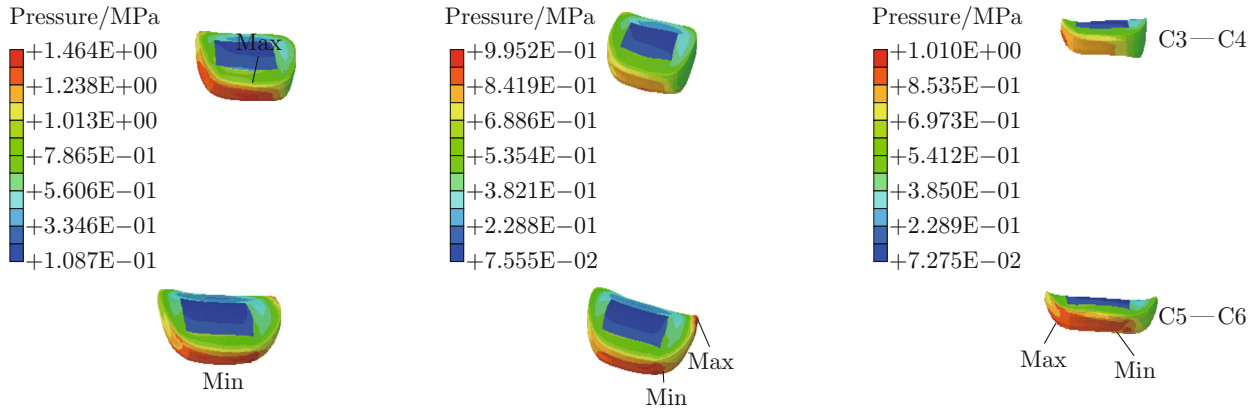

(c) Stress cloud plots of each condition at the C4—C5 segments implanted with Zero-P fusion

Fig. 3 Cloud plots of intradiscal pressure at adjacent segments after implantation of CP and Zero-P devices in C4—C5 under different working conditions

Table 5 Intradiscal pressure in adjacent segments after implantation of CP and Zero-P device in C5—C6

MPa

Segment	Flexion-extension			Lateral bending			Axial rotation		
	Normal	CP	Zero-P	Normal	CP	Zero-P	Normal	CP	Zero-P
C4—C5	1.69	2.03	1.79	1.04	1.32	1.19	1.00	1.27	1.18
C5—C6	1.37	—	—	0.87	—	—	0.96	—	—
C6—C7	1.08	1.85	1.28	0.74	1.41	0.84	0.72	1.36	0.88

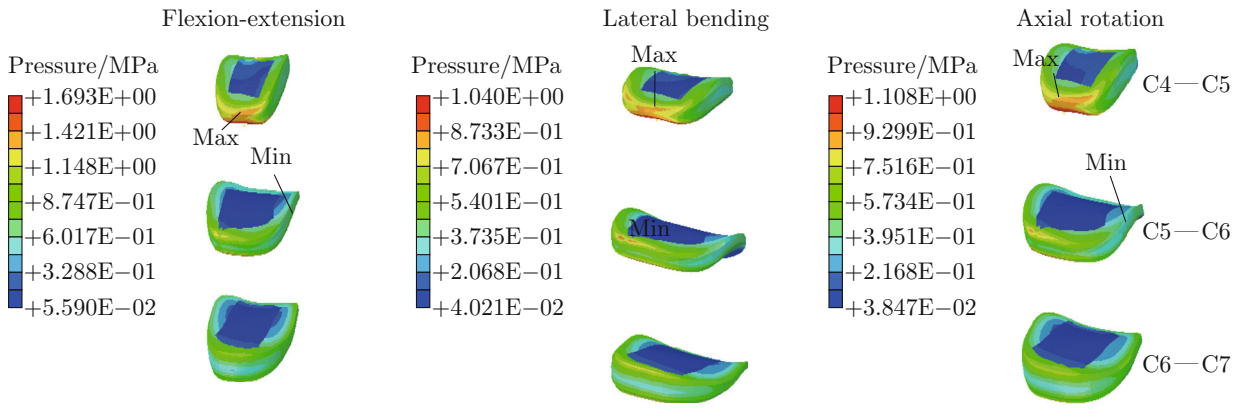

(a) Stress cloud plots showing the condition at intact cervical spine

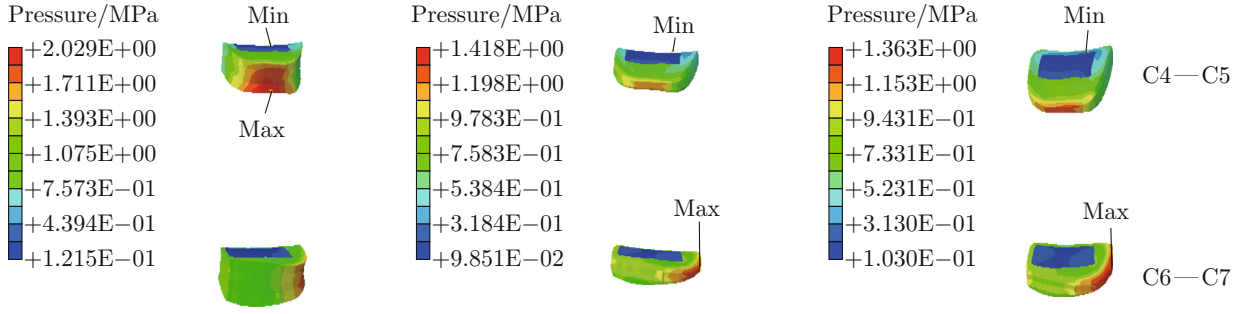

(b) Stress cloud plots showing the condition at the C5—C6 segments implanted with CP fusion

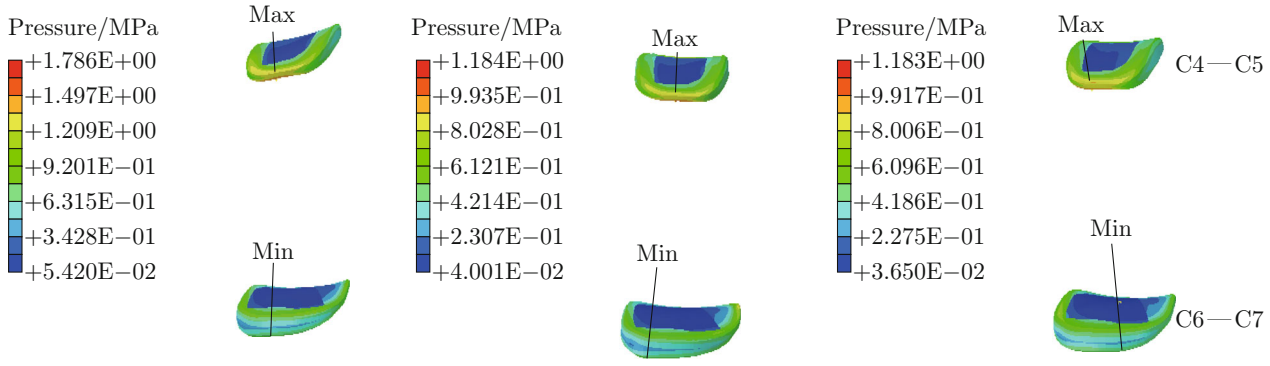

(c) Stress cloud plots showing the condition at the C5—C6 segments implanted with Zero-P fusion

Fig. 4 Cloud plots of intradiscal pressure at adjacent segments after implantation of CP and Zero-P device in C5—C6 under different operating conditions

3 Discussion

So far, whether ASD is caused by natural degeneration or cervical surgery remains unclear[5], abnormal ROM and intervertebral disc pressure at adjacent segments may be the primary cause of ASD[4]. Here, CP or Zero-P fusion systems were implanted into different cervical segments. After surgery, the ROM and intradiscal pressure of adjacent segments were evaluated using finite element analysis. The use of pure moments was performed to simulate the motion of the cervical spine in different working conditions, because pure moments offer two important advantages when evaluating spinal instrumentation in vitro: the pure moment applied to the spinal specimen can be applied equally to all segments of the specimen, and the pure moment can remain in the same direction as the spinal deformation during the test[23]. This loading method, moreover, has been recognized in different literature for relevant finite element analysis calculations. Therefore, the pure moment was also chosen for this study[9,11]. In the finite element analysis, the corresponding cervical vertebra model is used for simulation combined with the in vitro experiment of Panjabi et al.[23] and the relevant finite element experiment of Cao et al.[11]. In this study, the validity of the model was confirmed, and the results

confirmed that it is possible to use pure moments and the selected cervical vertebra model. Therefore, the results of the finite element calculation in this article are valid.

Clinical studies have shown that ACDF causes a significant reduction in the ROM of the implanted segment because the ROM of the implanted segment decreases dramatically. To restore the active response of the cervical spine, adjacent segments will compensate for increasing their ROMs, causing abnormal disc load, which may be an important reason for ASD[24-25]. Balaram et al.[26] reported that the ROM value at the fusion segment decreased sharply after using CP or Zero-P fusion system for ACDF in the cadaver cervical vertebra model, whereas that of adjacent segments increased to varying degrees. This work obtained similar results. Meanwhile, the segment mobility of the Zero-P fusion system is greater than that of the CP system, regardless of which segment the fusion is implanted in; except under the rotating condition, the adjacent segment ROM of the Zero-P fusion system becomes less than that of the CP system. Unlike the CP system, the Zero-P fusion system can effectively reduce the biomechanical response of adjacent segments and ensure the overall stability of the cervical spine.

Previous studies involving in vitro tests reveal that abnormal pressure in adjacent intervertebral discs after implantation of the fusion system may be another important factor for ASD development[27]. A nutrient exchange between the intervertebral disc and bone segment is heavily influenced by diffusion and osmotic gradient to a great extent. Therefore, the continuous increase of the pressure in the intervertebral disc may damage the nutrition diffusion, resulting in the deterioration of the intervertebral disc[28]. Eck et al.[29] found increased pressure in the adjacent intervertebral discs. In this study, the pressure in the adjacent intervertebral discs of the fusion segment was greater than that in the complete model after using the CP fusion system or the Zero-P fusion system for ACDF; the results were consistent with that of in vitro experiments. Meanwhile, when the fusion system is implanted into the C4—C5 segments, the intervertebral disc pressure of adjacent segments using the Zero-P fusion system is greater than that using the CP fusion system. In contrast, when the fusion system is implanted into the C5—C6 segments, the intervertebral disc pressure of adjacent segments using the Zero-P fusion system becomes lower than that using the CP fusion system. Therefore, in terms of the internal pressure changes of adjacent intervertebral discs, the performance of the two fusions had their advantages and disadvantages, with no significant difference.

This study has limitations. First, the complete cervical vertebra model and the two implant models did not consider muscle structure in the modeling process, which can not accurately simulate the cervical motion state, and may affect the finite element results. Additionally, all parameters selected in this study, including the angle of screw implantation and the design of the fusion system, were from the literature and assumptions. In this regard, changes in these factors may also influence the performance of the two fusion systems following cervical spine implantation. Thus, when these factors are combined, the biomechanical effects produced should be further studied.

4 Conclusion

For both CP and Zero-P fusion systems used for ACDF, fusion implant segment ROM decreases, whereas adjacent segment ROM and intervertebral disc pressure of adjacent segments increase. Unlike the Zero-P device system, the CP fusion system has a greater ROM loss in the implanted segment. The difference may be due to the lower stability of the Zero-P device than the CP system. Additionally, both have their advantages and disadvantages in the changes of intervertebral disc pressure at adjacent segments. If we analyze how to select a fusion system from two aspects, i.e., reducing the ROM of adjacent segments and abnormal pressure in the intervertebral disc, the Zero-P fusion system becomes the best option for ACDF of the C5—C6 segments. For the ACDF of the C4—C5 segments, a further comparison is required to select the most suitable fusion system. As an exploratory study, this work is not a direct guide to clinical surgery, but a biomechanical comparison between two fusion systems at different segments. Recommendations on biomechanics are hereby made for other researchers to conduct follow-up research. Therefore, the actual implantation effect of the two fusion systems warrants an additional clinical evaluation and investigation.

References

[1] BURKHARDT B W, BRIELMAIER M, SCHWERDTFEGER K, et al. Smith-Robinson procedure with and without Caspar plating as a treatment for cervical spondylotic myelopathy: A 26-year follow-up of 23 patients [J]. *European Spine Journal*, 2017, **26**: 1246-1253.

[2] YANG J J, YU C H, CHANG B S, et al. Subsidence and nonunion after anterior cervical interbody fusion using a stand-alone polyetheretherketone (PEEK) cage [J]. *Clinics in Orthopedic Surgery*, 2011, **3**(1): 16-23.

[3] HILIBRAND A S, ROBBINS M. Adjacent segment degeneration and adjacent segment disease: The consequences of spinal fusion? [J]. *The Spine Journal: Official Journal of the North American Spine Society*, 2004, **4**(6 Suppl): 190S-194S.

[4] ARUN R, FREEMAN B J C, SCAMMELL B E, et al. 2009 ISSLS Prize Winner: What influence does sustained mechanical load have on diffusion in the human

intervertebral disc? An *in vivo* study using serial post-contrast magnetic resonance imaging [J]. *Spine*, 2009, **34**(21): 2324-2337.

[5] CHUNG J Y, PARK J B, SEO H Y, et al. Adjacent segment pathology after anterior cervical fusion [J]. *Asian Spine Journal*, 2016, **10**(3): 582-592.

[6] CHEN Y Y, LIU Y, CHEN H J, et al. Comparison of curvature between the zero-P spacer and traditional cage and plate after 3-level anterior cervical discectomy and fusion: Mid-term results [J]. *Clinical Spine Surgery*, 2017, **30**(8): E1111-E1116.

[7] VANEK P, BRADAC O, DELACY P, et al. Anterior interbody fusion of the cervical spine with Zero-P spacer: Prospective comparative study-clinical and radiological results at a minimum 2 years after surgery [J]. *Spine*, 2013, **38**(13): E792-E797.

[8] ZHANG T X, GUO N N, GAO G, et al. Comparison of outcomes between Zero-p implant and anterior cervical plate interbody fusion systems for anterior cervical decompression and fusion: A systematic review and meta-analysis of randomized controlled trials [J]. *Journal of Orthopaedic Surgery and Research*, 2022, **17**(1): 1-9.

[9] HUA W B, ZHI J G, KE W C, et al. Adjacent segment biomechanical changes after one- or two-level anterior cervical discectomy and fusion using either a zero-profile device or cage plus plate: A finite element analysis [J]. *Computers in Biology and Medicine*, 2020, **120**: 103760.

[10] FAIZAN A, GOEL V K, GARFIN S R, et al. Do design variations in the artificial disc influence cervical spine biomechanics? A finite element investigation [J]. *European Spine Journal*, 2012, **21**(5): 653-662.

[11] CAO F, FU R C, WANG W Y. Comparison of biomechanical performance of single-level triangular and quadrilateral profile anterior cervical plates [J]. *PLoS One*, 2021, **16**(4): e0250270.

[12] HONG-WAN N, EE-CHON T, ZHANG Q H. Biomechanical effects of C2–C7 intersegmental stability due to laminectomy with unilateral and bilateral facetectomy [J]. *Spine*, 2004, **29**(16): 1737-1745.

[13] HSU C C, CHANG T K, HUY D C. Biomechanical comparison of different vertebral plate designs for anterior cervical discectomy and fusion using nonlinear C3-T2 multi-level spinal models [J]. *Computer-Aided Design and Applications*, 2015, **12**(2): 226-231.

[14] KWON J W, BANG S H, KWON Y W, et al. Biomechanical comparison of the angle of inserted screws and the length of anterior cervical plate systems with allograft spacers [J]. *Clinical Biomechanics*, 2020, **76**: 105021.

[15] NISHIZAWA S, YOKOYAMA T, YOKOTA N, et al. High cervical disc lesions in elderly patients - presentation and surgical approach [J]. *Acta Neurochirurgica*, 1999, **141**(2): 119-126.

[16] ZOU X N, XUE Q Y, LI H S, et al. Effect of alendronate on bone ingrowth into porous tantalum and carbon fiber interbody devicesAn experimental study on spinal fusion in pigs [J]. *Acta Orthopaedica Scandinavica*, 2003, **74**(5): 596-603.

[17] LIU N, LU T, WANG Y B, et al. Effects of new cage profiles on the improvement in biomechanical performance of multilevel anterior cervical corpectomy and fusion: A finite element analysis [J]. *World Neurosurgery*, 2019, **129**: e87-e96.

[18] MERCER S, BOGDUK N. The ligaments and anulus fibrosus of human adult cervical intervertebral discs [J]. *Spine*, 1999, **24**(7): 619-626.

[19] WEI W, LIAO S H, SHI S Y, et al. Straightened cervical lordosis causes stress concentration: A finite element model study [J]. *Australasian Physical & Engineering Sciences in Medicine*, 2013, **36**(1): 27-33.

[20] HUSSAIN M, NASSR A, NATARAJAN R N, et al. Biomechanics of adjacent segments after a multilevel cervical corpectomy using anterior, posterior, and combined anterior-posterior instrumentation techniques: A finite element model study [J]. *The Spine Journal*, 2013, **13**(6): 689-696.

[21] GOEL V K, CLAUSEN J D. Prediction of load sharing among spinal components of a C5-C6 motion segment using the finite element approach [J]. *Spine*, 1998, **23**(6): 684-691.

[22] LEE S H, IM Y J, KIM K T, et al. Comparison of cervical spine biomechanics after fixed- and mobile-core artificial disc replacement: A finite element analysis [J]. *Spine*, 2011, **36**(9): 700-708.

[23] PANJABI M M, CRISCO J J, VASAVADA A, et al. Mechanical properties of the human cervical spine as shown by three-dimensional load–displacement curves [J]. *Spine*, 2001, **26**(24): 2692-2700.

[24] ZHANG Q H, TEO E C, NG H W, et al. Finite element analysis of moment-rotation relationships for human cervical spine [J]. *Journal of Biomechanics*, 2006, **39**(1): 189-193.

[25] XIE N, YUAN W, YE X J, et al. Anterior cervical locking plate-related complications; prevention and treatment recommendations [J]. *International Orthopaedics*, 2008, **32**(5): 649-655.

[26] BALARAM A K, GHANAYEM A J, O'LEARY P T, et al. Biomechanical evaluation of a low-profile, anchored cervical interbody spacer device at the index level or adjacent to plated fusion [J]. *Spine*, 2014, **39**(13): E763-E769.

[27] CHANG U, KIM D H, LEE M C, et al. Changes in adjacent-level disc pressure and facet joint force after cervical arthroplasty compared with cervical discectomy and fusion [J]. *Journal of Neurosurgery Spine*, 2007, **7**(1): 33-39.

[28] GALBUSERA F, BRAYDA-BRUNO M, WILKE H J. Is post-contrast MRI a valuable method for the study of the nutrition of the intervertebral disc? [J]. *Journal of Biomechanics*, 2014, **47**(12): 3028-3034.

[29] ECK J C, HUMPHREYS S C, LIM T H, et al. Biomechanical study on the effect of cervical spine fusion on adjacent-level intradiscal pressure and segmental motion [J]. *Spine*, 2002, **27**(22): 2431-2434.